Highly efficient differentiation of hESCs to functional hepatic endoderm requires ActivinA and Wnt3a signaling

David C. Hay*†, Judy Fletcher*, Catherine Payne*, John D. Terrace*, Ronald C. J. Gallagher*, Jan Snoeys‡, James R. Black*, Davina Wojtacha*, Kay Samuel*, Zara Hannoun*, Anne Pryde*, Celine Filippi*, Ian S. Currie*, Stuart J. Forbes*, James A. Ross*, Philip N. Newsome§¶, and John P. Iredale*¶

*Medical Research Council Centre for Regenerative Medicine, University of Edinburgh, Edinburgh EH16 4SB, United Kingdom; ‡Johnson & Johnson Pharmaceutical Research and Development, B-2340 Beerse, Belgium; and §Institute of Biomedical Research, University of Birmingham, Edgbaston, Birmingham, B15 2TT, United Kingdom

Communicated by Ian Wilmut, University of Edinburgh, Edinburgh, United Kingdom, July 7, 2008 (received for review January 1, 2008)

Human embryonic stem cells (hESCs) are a valuable source of pluripotential primary cells. To date, however, their homogeneous cellular differentiation to specific cell types *in vitro* has proven difficult. Wnt signaling has been shown to play important roles in coordinating development, and we demonstrate that Wnt3a is differentially expressed at critical stages of human liver development *in vivo*. The essential role of Wnt3a in hepatocyte differentiation from hESCs is paralleled by our *in vitro* model, demonstrating the importance of a physiologic approach to cellular differentiation. Our studies provide compelling evidence that Wnt3a signaling is important for coordinated hepatocellular function *in vitro* and *in vivo*. In addition, we demonstrate that Wnt3a facilitates clonal plating of hESCs exhibiting functional hepatic differentiation. These studies represent an important step toward the use of hESC-derived hepatocytes in high-throughput metabolic analysis of human liver function.

definitive endoderm | function | hepatocyte | drug metabolism | high throughput

Human embryonic stem cells (hESCs) are derived from the inner cell mass of preimplantation embryos and demonstrate pluripotency *in vitro* and *in vivo* (1, 2). Such attributes allow hESCs to be differentiated down all germ lineages in large numbers and offer significant advantages over their adult stem cell counterparts, which are generally limited in their capacity to differentiate and proliferate (3). Although these hESCs provide a valuable source of adult differentiated cells, homogeneous cellular differentiation to specific germ layers has proven difficult to achieve. One potential explanation for this failure is that cells do not receive sequential developmental cues that they do *in vivo*.

Wnt signaling has been shown to play an important role in hESC self-renewal and differentiation and stimulates numerous intracellular signal transduction cascades, including the canonical pathway regulating gene expression in the nucleus and what seems to be a network of noncanonical pathways regulating many other aspects of cell biology [reviewed by Cadigan and Liu (4)]. In the absence of Wnt signaling, β-catenin is targeted for degradation; however, active Wnt signaling inhibits β-catenin destruction, resulting in its nuclear translocation (5, 6). After nuclear localization, β-catenin dimerizes with the nuclear proteins from the T cell factor/lymphoid enhancer factor (TCF/LEF) family and transactivates gene expression. TCF/LEFs are not only present in transcriptional activator complexes; they also play a role in corepressor complex assembly (6).

The important role played by Wnt signaling during gastrulation *in vivo* is evidenced by gene knockouts or dominant negatives (7, 8). Wnt3-mediated Brachyury expression is also important for migration of precursor cells through the anterior region of the primitive streak (PS). The subsequent specification of the anterior region of the PS to mesoderm or endoderm is likely to depend on the duration and magnitude of Nodal signaling (9, 10). Following its commitment the definitive endoderm (DE) lines the ventral region of the developing embryo and is patterned by adjacent mesenchyme. Liver formation depends on 2 mesenchymal structures, the cardiac mesoderm and septum transversum, which provide convergent instructive signals [reviewed by Zaret (11)].

ESCs have also been used as a cellular resource for modeling human development *in vitro*. These experiments demonstrated that the endodermal cell fate is based on the ability of a bipotential precursor, mesendoderm, to interpret different levels of Activin/Nodal signaling (12–16). In recent years there has been considerable focus on generating hepatic endoderm from ESCs. The differentiation of ESCs to hepatocytes has been shown to occur spontaneously after embryoid body formation (17–21) or directly using stagewise processes (19, 22, 23). Although there have been improvements in efficiencies, current strategies still yield relatively heterogeneous populations.

In this study, we demonstrate that Wnt3a is expressed at critical stages of human liver development *in vivo*, highlighting its important role in development. To study this further and model hESC differentiation through hepatocellular precursors, we have used Wnt3a *in vitro*. We demonstrate that Wnt3a elicits a rapid and highly efficient cellular progression through the PS to definitive and hepatic endoderm. The synergistic effect of Wnt3a and ActivinA on hESCs produced a viable and predictable model of human hepatic differentiation *in vitro* and *in vivo*. Additionally, Wnt3a promotes hepatocyte-like cell (HLC) functionality and facilitates clonal plating of hESCs capable of hepatic differentiation and function. These results represent an important step toward the use of hESC-derived HLCs in biomedical applications and high-throughput drug toxicity studies.

Results

Wnt3a Plays an Important Role in Developing Human Liver. During development the liver is formed from DE. The coordination of

Author contributions: D.C.H. and J.P.I. designed research; D.C.H., J.F., C.P., and J.D.T. performed research; D.C.H., J.F., C.P., J.D.T., R.C.J.G., J.S., J.R.B., D.W., K.S., Z.H., A.P., C.F., I.S.C., S.J.F., J.A.R., and J.P.I. contributed new reagents/analytic tools; D.C.H., J.F., C.P., J.D.T., R.C.J.G., J.S., J.R.B., D.W., K.S., Z.H., and A.P. analyzed data; and D.C.H., P.N.N., and J.P.I. wrote the paper.

The authors declare no conflict of interest.

Freely available online through the PNAS open access option.

†To whom correspondence should be addressed at: Medical Research Council Centre for Regenerative Medicine, University of Edinburgh, 49 Little France Crescent, Edinburgh EH16 4SB, Scotland, United Kingdom. E-mail: davehay@talktalk.net.

¶P.N.N. and J.P.I. contributed equally to this work.

This article contains supporting information online at www.pnas.org/cgi/content/full/0806522105/DCSupplemental.

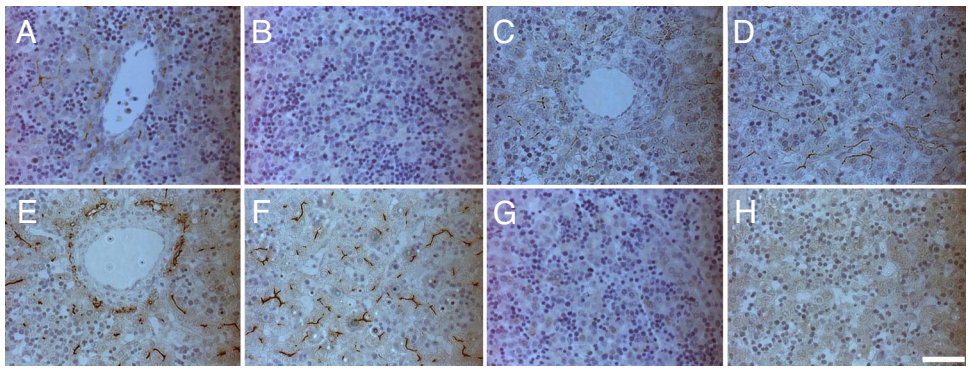

Fig. 1. Wnt3a and dipeptidyl peptidase IV (DPPIV) immunostaining in human T1 and T2 embryonic liver. Wnt3a expression was pronounced in areas near developing portal structures (*A*) but absent from the parenchyma (*B*) in T1 liver. In contrast, Wnt3a expression was detected in portal and parenchymal regions in T2 liver (*C* and *D*). DPPIV is a bile duct marker, and we it used as a positive control of bile duct localization. DPPIV expression was detected in both portal and parenchymal regions in T2 (*E* and *F*) sections. Immunostaining controls (*G* and *H*) stained negative, thereby demonstrating specificity. Immunohistochemistry images were captured using a Nikon TE300/U. (Scale bar, 100 μM.)

cell signaling during this process is critical for normal liver development. Wnt signaling plays an essential role in embryonic development and cellular differentiation, and we were interested in studying the instructive role played by Wnt during human liver development. Wnt3a expression was examined in first (T1) and second (T2) trimester human liver sections by immunostaining. T1 liver exhibited Wnt3a staining adjacent to developing portal structures but was not detected in the parenchyma (Fig. 1 *A* and *B*). However, in T2 livers the pattern of expression was both portal and parenchymal, suggesting that Wnt3a parenchymal expression correlated with, and possibly influenced, hepatocyte differentiation in the developing liver (Fig. 1 *C–F*), suggesting a possible role in early hepatocyte differentiation. As a control for specificity we used a negative control throughout our immunostaining (Fig. 1 *G* and *H*).

hESC Transition Through the PS Is Accelerated by Wnt3a and ActivinA Treatment. Mesoderm and endoderm are formed from a common precursor, mesendoderm. We were interested in the role that Wnt3a and ActivinA played throughout gastrulation and ultimately DE specification. Human endoderm differentiation was initiated using either ActivinA plus Wnt3a (AW) [supporting information (SI) Fig. S1] or ActivinA plus sodium butyrate (AB). hESCs were treated with AW for the first 3 days of the experiment and developed marked changes in their cellular morphology from day 1. AW-differentiated hESCs displayed loose colony structure 24 h after treatment, (Fig. S1*D*), and by days 2 and 3, differentiating cells had formed a confluent monolayer with some overgrowth detected, the majority of which was lost during subsequent phases of the cellular differentiation (Fig. S1 *E* and *F*). In contrast, hESCs incubated with AB displayed a much looser colony structure, not forming a confluent monolayer until day 3 (Fig. S1 *J–L*) Of note, the areas of overgrowth present in these cultures continued to grow throughout subsequent phases of differentiation.

Consistent with changes in cell morphology, we observed changes in gene expression. hESCs and differentiating cells were immunostained for the PS marker Brachyury. Brachyury expression, absent in hESCs (Fig. S1*B*), was detected in 96% ± 0.3% of cells treated with AW by day 1 (Fig. S1*G*) and decreased on days 2 and 3, indicating cellular transition through the PS (Fig. S1 *H* and *I*). Cells treated with AB, however, exhibited a different pattern, with all cells expressing Brachyury for the first 3 days, suggesting slower progress through the PS (Fig. S1 *M–O*). The specificity of immunostaining was confirmed using an IgG-negative control (Fig. S1*C*).

To fully assess cellular transition through the PS we used a panel of lineage-specific PCR markers, which were compared with and quoted as fold induction over hESC levels. The profile of Brachyury gene expression in AW cells was in line with immunostaining and confirmed more rapid cellular progression through the PS (Fig. S2*A*, AW1–3) than AB cells (Fig. S2*A*, AB1–3). The differential regulation of the Brachyury was paralleled by the expression of endodermal markers *SOX17* and *HNF3β*. *SOX17* and *HNF3β* levels were induced earlier in AW-treated cells (Fig. S2*B*, AW1–3) than in AB-treated cells (Fig. S2*B*, AB1–3). The decrease in *Brachyury* and faster induction of *SOX17* and *HNF3β* suggests that cells treated with AW transit more rapidly through the PS than cells treated with AB. To confirm cellular commitment to DE we assessed *NODAL* and *CRIPTO* expression. Both treatment groups exhibited similar patterns of expression, with entry into DE at day 3 (Fig. S2 *D* and *E*). Consistent with hESC differentiation toward the endoderm, we observed a decrease in *OCT4* levels as differentiation proceeded in both treatment groups (Fig. S2*F*).

Wnt Signaling Plays an three Important Role in PS Formation and Endoderm Specification. At least three Wnts are required for different aspects of gastrulation. *WNT3* and *WNT3a* are expressed in the PS of mouse and are required for mesoderm formation (24), whereas *WNT11* is expressed in the blastopore of *Xenopus* and zebrafish and is thought to be involved in controlling extension movements in gastrulation (25). *WNT3*, *WNT3a*, and *WNT11* levels were measured during PS and endoderm formation. In line with *BRACHYURY*, *WNT3a* expression was maximal at day 1 in AW cells (Fig. 2*A*, AW1) and decreased during days 2 and 3 (Fig. 2*A*, AW2 and AW3), indicating that the formation of and transition through the PS was proceeding normally. Cells differentiated with AB exhibited a different pattern, with peak levels of *WNT3a* detected at day 2 (Fig. 2*A*, AB1–3). In both treatment groups the *WNT3* induction profile was similar throughout the PS transition, indicating that *WNT3* was important for PS and endoderm development (Fig. 2*B*, AW1–3 and AB1–3). Similarly, *WNT11* was induced in both AW and AB cultures over the 3-day time course (Fig. 2*C*, AW1–3 and AB1–3), consistent with its role in regulating gastrulation. Of note, the high levels of *WNT11* expression coincided with the expression of endodermal markers *SOX17*, *HNF3β*, *NODAL*, and *CRIPTO* in both models.

AW-Driven hESC Differentiation Induces Rapid and Homogeneous Hepatic Endoderm Differentiation. In addition to a role for Wnt3a in facilitating endoderm differentiation, we also the studied capability of those endodermal cell populations to form hepatic

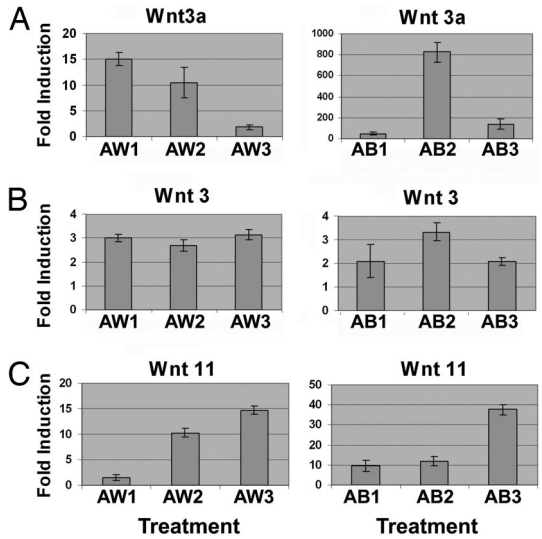

Fig. 2. Wnt signaling pathways play an important role in endoderm specification. (*A*) *WNT3a* is down-regulated in response to AW throughout differentiation (AW1–3). *WNT3a* is dramatically up-regulated in response to AB before down-regulation (AB1–3). (*B*) Levels of *WNT3* are unchanged from days 1 to 3 in response to AW and AB (AW1–3 and AB1–3). (*C*) *WNT11* is up-regulated in response to both AW and AB, coinciding with a decrease in *WNT3a* (AW1–3 and AB1–3). qPCR amplicons were measured using an ABI Prism 7900. AW1–3, AW-treated cells on days 1, 2, or 3; AB1–3, AB-treated cells on days 1, 2, or 3. (Scale bar, 100 μM.)

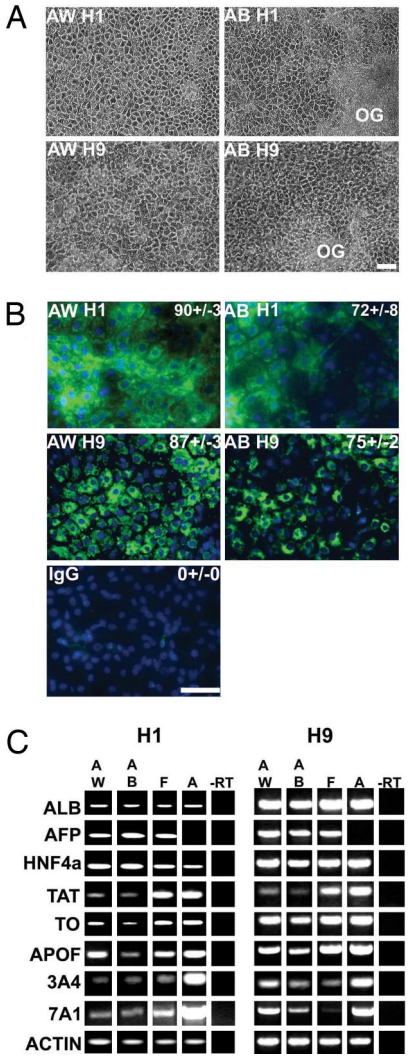

Fig. 3. Wnt3a plus ActivinA promotes increased hepatocytic differentiation of hESCs. (*A*) Cellular morphology at day 10 in AW- and day 14 in AB-differentiated H1 and H9 hESC lines. Cells produced by AW show very little overgrowth (OG) compared with cells produced by AB. (*B*) More efficient generation of albumin-positive hepatocytes from hESCs using AW (≈90% H1 and ≈87% H9) than AB (≈72% H1 and ≈75% H9). IgG staining was used as a negative control. Immunostaining was recorded using a Leica DMIRB. (Scale bar, 100 μM.) Results are presented as a mean of four fields of view ± SE. (*C*) Gene expression of *in vitro*-derived cells were examined using semiquantitative PCR. ALB, albumin; AFP, α fetoprotein; HNF4α, hepatocyte nuclear factor 4 α; TAT, tyrosine amino transferase; TO, tryptophan dioxygenase; APOF, apolipoprotein F; 3A4, cytochrome p450 3A4; 7A1, cytochrome p450 7A1; Actin, β-actin; F, fetal liver cDNA; A, adult liver cDNA.

endoderm. Cells treated with AW or AB were transferred to other types of media known to specify hepatic endoderm (23). Cells primed with AW exhibited hepatocyte morphology by day 10 (Fig. 3*A*, AW H1 and AW H9), in contrast with cells differentiated with AB, which required 14 days' differentiation before they developed characteristic hepatocyte morphology (Fig. 3*A*, AB H1 and AB H9). In addition to the relative delay in hepatocyte appearance, we also detected many areas of overgrowth in AB cultures (Fig. 3*A*, AB H1 and AB H9). The number of hESC-derived hepatocytes in culture was assessed morphologically, by their polygonal shape and prominent nucleoli, and confirmed by albumin staining. The differentiation of H1 hESCs using AW yielded 90% ± 3% albumin-positive hepatocytes (Fig. 3*B*, AW H1) on day 17, compared with 72% ± 8% of albumin-positive cells seen in response to AB (Fig. 3*B*, AB H1) on day 17. We also tested an independent hESC line, H9, and demonstrated that AW and AB treatment elicited similar amounts of human hepatocyte differentiation (Fig. 3*B*, AW H9 and AB H9). Specificity of immunostaining was confirmed using an IgG-negative control (Fig. 3*B*, IgG). Cells were maintained in culture to day 18, and their gene expression was analyzed by RT-PCR (Fig. 3*C*). Our results show that H1 or H9 cells differentiated by either method expressed *CYP7A1*, seen in liver but not yolk sac, and a repertoire of hepatocyte markers: *ALB*, *AFP*, *HNF4α*, TAT, TO, APOF, and *CYP3A4*.

AW-Driven hESC Differentiation Produces HLCs That Express a Wide Variety of Hepatocyte-Specific Functions. In addition to marker expression, we studied hESC-derived hepatocyte functionality. hESC-derived AW and AB HLCs (AWHLCs and ABHLCs, respectively) were matured using either L-15 (26) or Eagle's Minimal Essential Medium (MEME) in the presence or absence of a mixture known to induce hepatocyte function *in vitro* (27). After incubation, hepatocyte metabolism was measured by 2 assays, ureagenesis and gluconeogenesis. AWHLCs matured in either L-15 or MEME plus lactate, pyrurate, octanoate, and ammonium chloride (LPON) exhibited greater urea production than their ABHLC counterparts (Fig. 4*A*). hESC-derived hepatocytes from either protocol exhibited a similar pattern of gluconeogenesis, which was enhanced in the presence of LPON (Fig. 4*B*). Liver synthetic function was measured using ELISA. In addition to α fetoprotein (AFP), other proteins included fibrinogen, fibronectin, thyroxin-binding prealbumin (TBPA), and haptoglobin. AWHLCs secreted greater amounts of AFP (Fig. 4*C*), fibrinogen (Fig. 4*D*), and TBPA (Fig. 4*E*) than ABHLCs. The production of fibronectin (Fig. 4*F*), haptoglobin, and albumin (Fig. 4*G*) was similar in both treatment groups.

AW-Differentiated HLCs Engraft *in Vivo* and Are More Functional than ABHLCs. A criticial ability of hESC-derived hepatocytes to engraft into the spleen was examined *in vivo* using NOD*scid* mice.

CELL BIOLOGY

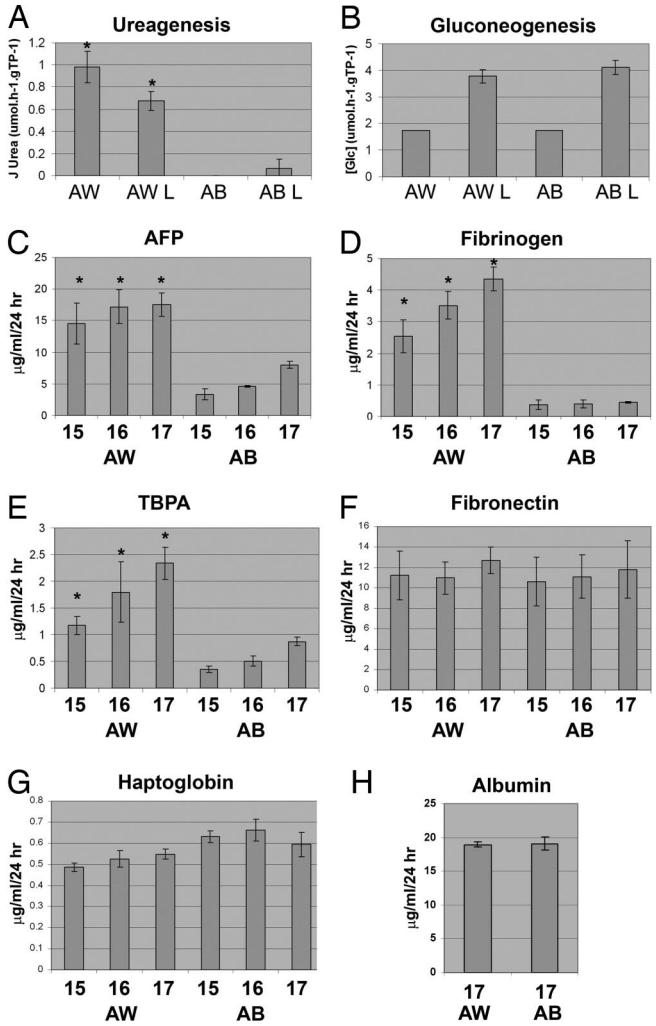

Fig. 4. AWHLCs display increased human liver function *in vitro*. (*A*) Urea synthesis, J Urea (μmol·h^{-1}·gTP^{-1}), was measured from cells derived from both AW and AB protocols. hESC-derived hepatocytes differentiated with AW exhibited greater urea production than cells differentiated with AB. (*B*) Gluconeogenesis was comparable in both treatment groups. Gluconeogenesis, [Glc] (umol·h^{-1}·gTP^{-1}), was greater in cells treated with LPON (L). (*C–G*) Serum protein production was measured by ELISA on days 15, 16, and 17, and units are quoted as μg/24 h. AW-differentiated cells exhibited greater production of AFP, fibrinogen, and TBPA than AB cells. *, $P < 0.01$ by Student's *t* test. HLCs from both protocols exhibited similar levels of fibronectin, haptoglobin, and albumin, ($n = 6$). (*H*) Albumin protein production was measured by ELISA on day 17, and units are quoted as μg/24 hr.

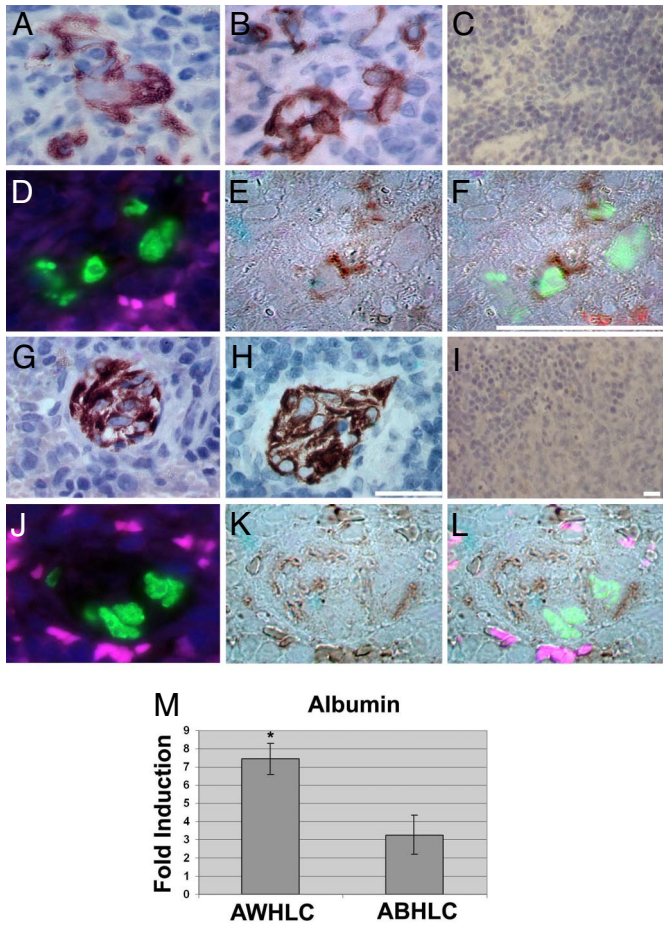

Fig. 5. AW and AB HLCs engraft in the spleen and liver *in vivo*. (*A* and *B*) Clusters of AW-derived hepatocytes expressing CK18 (*A*) and CK19 (*B*) in the spleen. (*C*) IgG control. (*D*) Clusters of AW-derived hepatocytes detected by FISH. (*E*) Human cells express albumin in the spleen. (*F*) FISH/immunostaining overlay. (*G* and *H*) Clusters of AB-derived hepatocytes expressing (*G*) CK18 and (*H*) CK19 in the spleen. (*I*) IgG controls. (*J*) Clusters of AW-derived hepatocytes detected by FISH. (*K*) Human cells express albumin in the spleen. (*L*) FISH/immunostaining overlay. (*M*) Transplanted AW and AB HLCs express albumin *in vivo* as detected by ELISA. The results presented are a mean of four animals ± SE. *, $P < 0.01$ by Student's *t* test. Phase images were recorded using a Zeiss Axioplan fluorescent microscope. (Scale bar, 100 μM.) Immunostaining was recorded using a Zeiss Axioplan fluorescent microscope.

hESC-derived HLCs (10^6) were injected intrasplenically into adult mice (aged 8–10 weeks). Three days after injection the animals were killed, and the presence of hESC-derived hepatocytes was detected using human-specific CK18, CK19, human FISH, and albumin staining. Clusters of AW-derived human CK18- and CK19-positive HLCs were detected in the spleen of recipient animals (Fig. 5 *A–C*). Hepatocytes present in the spleen also stained positive for human DNA by FISH, which colocalized with albumin staining, demonstrating hepatocellular function *in vivo* (Fig. 5 *D–F*). In addition to AWHLCs, clusters of ABHLCs exhibiting the above attributes were also detected in the spleen of recipient animals (Fig. 5 *G–L*). Human albumin production in mouse serum was measured using ELISA. ELISA serum absorbance values for mice with AWHLCs engrafted were ≈7.5-fold greater than those for control mice, whereas for ABHLCs values were ≈3.3-fold greater than those of control mice. These results indicate either that AWHLCs are a more functional cell population or that a greater number of cells proliferated or engrafted *in vivo*.

Wnt3a Treatment Facilitates Single-Cell Cloning of hESCs Capable of HLC Differentiation and Function *in Vitro*. Because AWHLCs exhibited a broader range of hepatic function than ABHLCs, AWHLCs were used in p450 metabolic studies. Cytochrome p450s metabolize both exogenous and endogenous compounds, accounting for their central importance in human health. hESC-derived HLCs displayed CYP1A2 (0.012 ± 0.002 pmol/min·mg protein) metabolic activity that could be assayed in 12-well format (Fig. 6*A*). The ability to move models of liver function, in particular p450 metabolism, to a high-throughput format is attractive to drug toxicology testing programs. In an attempt to provide high-throughput format models, we studied the ability of hESC to plate as small colonies that could be seeded into 96-well plates. Wnt3a pretreatment of hESCs (whESC) promoted hESCs self-renewal, and after passaging, hESCs displayed looser and smaller colony structure than nontreated hESCs. We reasoned that if hESCs could self-renew in

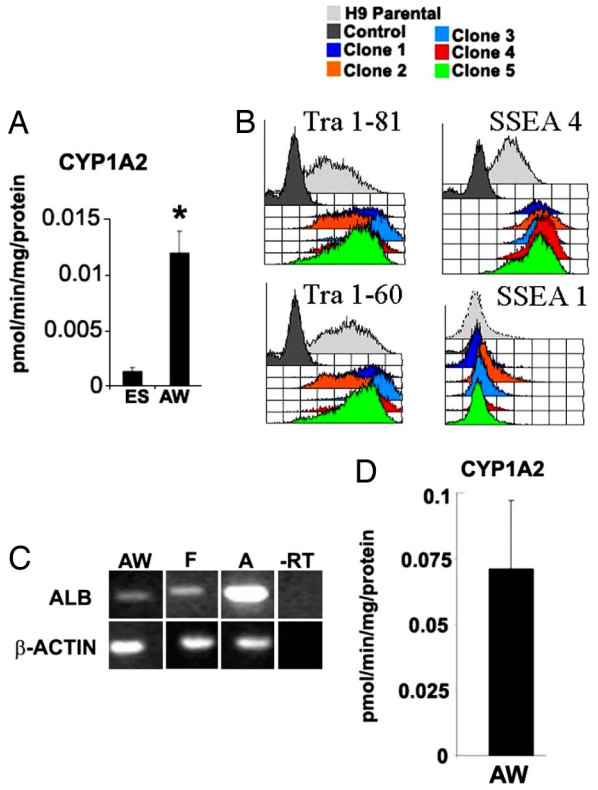

Fig. 6. Wnt treatment of hESCs promotes p450 function and high-throughput screening *in vitro*. (*A*) hESCs (ES) and AWHLCs (AW) were incubated with substrate for 24 h. After incubation cellular supernatants were harvested, and metabolite production was determined by mass spectrometry (Thermo Electron), normalized to protein levels, and expressed as pmol/min·mg protein. AWHLC displayed greater CYP1A2 metabolism than ES cells ($n = 3$). (*B*) hESCs were treated with Wnt3a, single-cell cloned in 96-well plates and expanded *in vitro*. After 10 passages, ES cell-surface markers were analyzed by FACS. Single-cell cloned hESCs retained expression of hESC markers SSEA4, Tra1–60, and Tra1–81 and did not express SSEA1, a marker of hESC differentiation. (*C*) Clonally plated hESCs could be differentiated to HLCs in 96-well plates. Cells that exhibited HLC morphology also expressed albumin *in vitro*. (*D*) AW-treated hESCs differentiated to HLCs exhibited CYP1A2 metabolic activity, which could be assayed in 96-well plate format *in vitro* ($n = 10$). *, $P < 0.01$ by Student's *t* test.

smaller colonies, they may also tolerate single-cell cloning. To test our hypothesis we seeded 96-well plates with single whESCs and grew them to confluence. Five whESC clones, selected from 50, were expanded and passaged 10 times before hESC identity and differentiation potential were assessed using FACS (Fig. 6*B*). Clonally derived hESC expressed the correct repertoire of hESC cell-surface markers (SSEA4, Tra1–60, and Tra1–81), expressed Oct-4, and were capable of forming embryo bodies exhibiting cell types from all three germ layers. In addition to hESC self-renewal and pluripotentiality, we tested clonally derived lines' ability to differentiate toward hepatic endoderm. AW-driven hepatocyte differentiation was carried out as before, and hepatic identity was assessed by morphology, albumin expression, and CYP1A2 metabolic activity (0.071 ± 0.026 pmol/min·mg protein) indicative of scalable hepatic differentiation and high-throughput function *in vitro*. The HLCs were compared with freshly isolated human hepatocytes. Populations of HLCs derived in 12-well plates exhibited CYP1A2 activity equivalent to 4% of that observed from adult hepatocytes. In contrast, HLCs derived from clonal lines exhibited CYP1A2 activity at 24% of adult hepatocytes, demonstrating significantly improved drug metabolism.

Discussion

The results presented here demonstrate efficient and scalable human HLC generation *in vitro*. The exposure of hESCs, in a manner designed to mimic events in the developing embryo, resulted in their homogeneous hepatocellular differentiation and displayed increased hepatocellular function *in vitro* and *in vivo*. Wnt treatment, in addition to promoting cellular functionality, also facilitated the high-throughput study of human liver function *in vitro*.

The liver bud is formed from foregut endoderm during development. The generation of this structure begins with establishment of the PS and its derivative germ layers. Both Wnt and Activin signaling pathways have been shown to play important roles in mesoderm and endoderm specification (28–30). In addition, Wnt3a's expression in developing human liver made it a candidate factor for directing efficient hESC hepatocyte differentiation. Our second model, AB, was chosen for its ability to form relatively high levels of hepatic endoderm, and we reasoned that this would serve as an established comparative (31). Monolayers of hESCs were differentiated using the two models producing HLCs that express epithelial and biliary markers *in vitro* and *in vivo*, which mimics the phenotype of oval/progenitor cell *in vivo*. hESCs treated with AW promoted a more rapid transition through the PS than cells differentiated with AB. Of note, the dramatic increase in *WNT3a* and *BRACHYURY* at day 2 in AB cells could be responsible for the late induction of endoderm markers *SOX17* and *HNF3β*. The subsequent differentiation of DE to hepatic endoderm, using AW, was more rapid and promoted hepatic function *in vitro* and *in vivo*. In addition to its role in cellular differentiation, Wnt3a has also been studied in hESC single-cell plating. In a previous study Wnt3a promoted both cellular replating and differentiation and as a result was consequently was less effective than hESC clonal passaging (32). In contrast, our results demonstrate that Wnt3a treatment of hESCs promoted their single-cell dissociation and self-renewal, promoting undifferentiated hESC clonal passaging.

There are a number of signaling pathways involved in the complex cascade of events that lead to DE formation. In both our models, cells initially expressed genes indicative of PS formation and went on to express endodermal genes in a manner akin to human development. The induction of Brachyury by Wnt3a (24) and Sox17 by Nodal (33) are well documented and consistent with our observations. In addition, both Brachyury and Sox17 are known to be essential components in driving *WNT11* expression (34) and, in agreement with previous experiments, we demonstrate that increased *WNT11* expression is paralleled by a decrease in *WNT3A* and *BRACHYURY* expression (35). In effect, Wnt11 could be acting as a molecular switch responsible for the commitment of differentiating cells to DE. The mesendodermal-to-endodermal transition requires a fundamental change in cellular gene expression programs. Although we observe down-regulation of *BRACHYURY* and *WNT3A*, *WNT3* expression was still detectable, indicating that β-Catenin signaling, responsible for Cripto induction (36), is still active in differentiating cells. It may be the case that Wnt11-mediated shutdown of Wnt3a-driven β-Catenin/TCF signaling dampens down mesoderm formation and that Wnt3-driven β-Catenin signaling is respecified to an endodermal program of gene expression. With this in mind, it is interesting to note that Sox17 and β-catenin heterodimers have been shown to cooperate in the regulation of endodermal gene expression (37) and therefore may represent one of the Wnt11 effector complexes in endoderm specification.

In conclusion, we demonstrate the efficient generation of hESC-derived HLCs that differentiate through appropriate *in vivo* intermediates. This has led to the generation of a scalable liver differentiation model that bypasses the problems associated with sourcing and culturing primary human hepatocytes. Additionally, we predict that our high-throughput technology will not only be

important in the prediction of hepatotoxicity but will be extremely useful in the generation of other developmental testing models.

Materials and Methods

Cell Culture and Differentiation. hESCs (H1 and H9) were cultured and propagated as described (23, 38). Differentiation was initiated at 60–70% confluence, by replacing mouse embryomic fibroblast conditioned medium (MEF-CM) with differentiation medium (RPMI1640 containing 1× B27 (both from Invitrogen), 1 mM sodium butyrate (Sigma), and 100 ng/ml ActivinA (Peprotech) or 50 ng/ml Wnt3a (R&D Systems) and 100 ng/ml ActivinA. After 72 h (changing medium every day), differentiating cells were cultured in subsequent differentiation media as described in ref. 31.

RNA Isolation and RT-PCR. Total RNA was harvested from cells and underwent RT-PCR as described (23, 38). Total RNA from mouse tissue was isolated using RNeasy Plus mini kit (Qiagen 74134) as per the manufacturer's instructions. cDNA was generated using TaqMan reverse transcription reagent (Applied Biosystems N8080234). Quantitative PCR was carried out as described (39) and measured on an ABI Prism 7900 (Applied Biosystems. Optimized primer conditions for PCRs are shown in Tables S1 and S2.

Immunofluoresence and Immunohistochemistry. Monolayer cultures were fixed and stained as described (23). Human and mouse tissues were embedded in paraffin and 3-μm serial sections were cut. Sections were microwaved in the following heat retrieval methods: 10 mM Tris, DAKO target retrieval high pH (S3306), or 10 mM citrate buffer, incubated in 3% H_2O_2 for 5 min. Optimized concentrations of primary and secondary antibodies are shown in Table S3.

Measurement of Hepatocyte Export Proteins. Cells were cultured in 6-well plates in 1 ml of L-15, and after 24-h supernatants were collected for export protein assay. The hepatic export proteins were measured as described (27, 40, 41).

Measurement of Hepatocyte Metabolism. Hepatocyte metabolism was measured in the context of gluconeogenesis and ureagenesis as described (27). CYP1A2 activity was measured in 1 × 10^5 HLCs or freshly isolated human hepatocytes (Johnson & Johnson) using 2 μM 7-ethoxyresorufin in culture medium for 24 h at 37°C. Liberated resorufin was fluorometrically analyzed (excitation, 550 nm; emission, 585 nm) in a Safire spectrophotometer (Tecan) and reported as specific activity (pmol/min·mg protein) ± SEM.

Animals. Adult NOD.CB17-*Prkdc*^{scid}/J mice were purchased from the Jackson Laboratory and housed in individual ventilated cages. Experimental protocols were carried out in accordance with permits and guidelines issued by the University of Edinburgh Ethical Review Committee and the United Kingdom Home Office (Project Licence 60/2914). Cells were differentiated in the AW or the AB protocol for 10 or 14 days, respectively. Cells were harvested using trypsin-EDTA and filtered through a 100-mM filter. NODscid mice (aged 8–10 weeks) were injected intrasplenically with 1 × 10^6 cells after laparotomy.

FISH. Formalin-fixed, paraffin-embedded sections were dewaxed and rehydrated. The sections were then microwaved in 10 mM citrate buffer for 20 min and denatured in 70% formamide in 2× SSC for 3 min, dehydrated through 90–100% EtOH, and air dried digoxygenine (DIG)-labeled human genomic DNA (150 ng) was hybridized overnight at 37°C. Slides were washed 4 × 3 min in 2× SSC at 45°C, followed by 4 × 3 min in 0.1× SSC at 60°C. Slides were then incubated in FITC-labeled sheep anti-DIG for 30 min, washed 3 × 2 min in 4× SSC/0.1% Tween, and then incubated in FITC-labeled antisheep antibody for 30 min, washed 3 × 2 min in 4× SSC/0.1% Tween, mounted in Vectorshield DAPI (Vector Laboratories), and visualized using a Zeiss Axioplan fluorescent microscope.

Flow Cytometry. Optimized concentrations for flow cytometry were used as described (42).

ACKNOWLEDGMENTS. We thank Professor Sir Ian Wilmut for help in providing technical support. The monoclonal antibody SSEA4 was obtained from the Developmental Studies Hybridoma Bank, developed under the auspices of the National Institute of Child Health and Human Development, and maintained by the University of Iowa, Department of Biological Sciences (Iowa City, IA). The studies were cofunded by the University of Edinburgh and the Geron Corporation. R.C.J.G. was supported by the Chief Scientist's Office of the Scottish Executive (Grant CZG/1/137).

1. Reubinoff BE, Pera MF, Fong CY, Trounson A, Bongso A (2000) Embryonic stem cell lines from human blastocysts: Somatic differentiation *in vitro*. *Nat Biotechnol* 18:399–404.
2. Thomson JA, *et al.* (1998) Embryonic stem cell lines derived from human blastocysts. *Science* 282:1145–1147.
3. Czyz J, *et al.* (2003) Potential of embryonic and adult stem cells *in vitro*. *Biol Chem* 384:1391–1409.
4. Cadigan KM, Liu YI (2006) Wnt signaling: Complexity at the surface. *J Cell Sci* 119:395–402.
5. Kohn AD, Moon RT (2005) Wnt and calcium signaling: Beta-catenin-independent pathways. *Cell Calcium* 38:439–446.
6. Willert K, Jones KA (2006) Wnt signaling: Is the party in the nucleus? *Genes Dev* 20:1394–1404.
7. Tada M, Smith JC (2000) Xwnt11 is a target of *Xenopus* Brachyury: Regulation of gastrulation movements via Dishevelled, but not through the canonical Wnt pathway. *Development* 127:2227–2238.
8. Liu P, *et al.* (1999) Requirement for Wnt3 in vertebrate axis formation. *Nat Genet* 22:361–365.
9. Lowe LA, Yamada S, Kuehn MR (2001) Genetic dissection of nodal function in patterning the mouse embryo. *Development* 128:1831–1843.
10. Vincent SD, Dunn NR, Hayashi S, Norris DP, Robertson EJ (2003) Cell fate decisions within the mouse organizer are governed by graded Nodal signals. *Genes Dev* 17:1646–1662.
11. Zaret KS (2001) Hepatocyte differentiation: From the endoderm and beyond. *Curr Opin Genet Dev* 11:568–574.
12. Gadue P, Huber TL, Paddison PJ, Keller GM (2006) Wnt and TGFbeta signaling are required for the induction of an *in vitro* model of primitive streak formation using embryonic stem cells. *Proc Natl Acad Sci USA* 103:16806–16811.
13. Tada S, *et al.* (2005) Characterization of mesendoderm: A diverging point of the definitive endoderm and mesoderm in embryonic stem cell differentiation culture. *Development* 132:4363–4374.
14. D'Amour KA, *et al.* (2005) Efficient differentiation of human embryonic stem cells to definitive endoderm. *Nat Biotechnol* 23:1534–1541.
15. D'Amour KA, *et al.* (2006) Production of pancreatic hormone-expressing endocrine cells from human embryonic stem cells. *Nat Biotechnol* 24:1392–1401.
16. McLean AB, *et al.* (2007) Activin a efficiently specifies definitive endoderm from human embryonic stem cells only when phosphatidylinositol 3-kinase signaling is suppressed. *Stem Cells* 25:29–38.
17. Itskovitz-Eldor J, *et al.* (2000) Differentiation of human embryonic stem cells into embryoid bodies compromising the three embryonic germ layers. *Mol Med* 6:88–95.
18. Schuldiner M, Yanuka O, Itskovitz-Eldor J, Melton DA, Benvenisty N (2000) Effects of eight growth factors on the differentiation of cells derived from human embryonic stem cells. *Proc Natl Acad Sci USA* 97:11307–11312.
19. Rambhatla L, Chiu CP, Kundu P, Peng Y, Carpenter MK (2003) Generation of hepatocyte-like cells from human embryonic stem cells. *Cell Transplant* 12:1–11.
20. Lavon N, Yanuka O, Benvenisty N (2004) Differentiation and isolation of hepatic-like cells from human embryonic stem cells. *Differentiation* 72:230–238.
21. Duan Y, *et al.* (2007) Differentiation and enrichment of hepatocyte-like cells from human embryonic stem cells *in vitro* and *in vivo*. *Stem Cells.* 25:3058–3068.
22. Cai J, *et al.* (2007)Directed differentiation of human embryonic stem cells into functional hepatic cells. *Hepatology* 45:1229–1239.
23. Hay DC, *et al.* (2007) Direct differentiation of human embryonic stem cells to hepatocyte-like cells exhibiting functional activities. *Cloning Stem Cells* 9:51–62.
24. Yamaguchi TP, Takada S, Yoshikawa Y, Wu N, McMahon AP (1999) T (Brachyury) is a direct target of Wnt3a during paraxial mesoderm specification. *Genes Dev* 13:3185–3190.
25. Heisenberg CP, *et al.* (2000) Silberblick/Wnt11 mediates convergent extension movements during zebrafish gastrulation. *Nature* 405:76–81.
26. Mitchell AM, Bridges JW, Elcombe CR (1984) Factors influencing peroxisome proliferation in cultured rat hepatocytes. *Arch Toxicol* 55:239–246.
27. Filippi C, *et al.* (2004) Improvement of C3A cell metabolism for usage in bioartificial liver support systems. *J Hepatol* 41:599–605.
28. Hemmati-Brivanlou A, Melton DA (1992) A truncated activin receptor inhibits mesoderm induction and formation of axial structures in *Xenopus* embryos. *Nature* 359:609–614.
29. Hussain SZ, *et al.* (2004) Wnt impacts growth and differentiation in ex vivo liver development. *Exp Cell Res* 292:157–169.
30. Peifer M, Polakis P (2000) Wnt signaling in oncogenesis and embryogenesis—a look outside the nucleus. *Science* 287:1606–1609.
31. Hay DC, *et al.* (2008) Efficient differentiation of hepatocytes from human ESCs exhibiting markers recapitulating liver development *in vivo*. *Stem Cells* 26:894–902.
32. Hasegawa K, Fujioka T, Nakamura Y, Nakatsuji N, Suemori H (2006) A method for the selection of human embryonic stem cell sublines with high replating efficiency after single-cell dissociation. *Stem Cells* 12:2649–2660.
33. Sinner D, Rankin S, Lee M, Zorn AM (2004) Sox17 and beta-catenin cooperate to regulate the transcription of endodermal genes. *Development* 131:3069–3080.
34. Saka Y, Tada M, Smith JC (2000) A screen for targets of the *Xenopus* Tbox gene Xbra. *Mech Dev* 93:27–39.
35. Zhu H, *et al.* (2004) Analysis of Wnt gene expression in prostate cancer: Mutual inhibition by WNT11 and the androgen receptor. *Cancer Res* 64:7918–7926.
36. Morkel M, *et al.* (2003) Betacatenin regulates Cripto- and Wnt3-dependent gene expression programs in mouse axis and mesoderm formation. *Development* 130:6283–6294.
37. Liu Y, *et al.* (2007) Sox17 is essential for the specification of cardiac mesoderm in embryonic stem cells. *Proc Natl Acad Sci USA* 104:3859–3864.
38. Hay DC, Sutherland L, Clark J, Burdon T (2004) Oct-4 knockdown induces similar patterns of endoderm and trophoblast differentiation markers in human and mouse embryonic stem cells. *Stem Cells* 22:225–235.
39. Holland PM, Abramson RD, Watson R, Gelfand DH (1991) Detection of specific polymerase chain reaction product by utilizing the 5′—3′ exonuclease activity of Thermus aquaticus DNA polymerase. *Proc Natl Acad Sci USA* 88:7276–7280.
40. O'Riordain MG, *et al.* (1995) Insulin and counterregulatory hormones influence acute-phase protein production in human hepatocytes. *Am J Physiol* 269:E323–E330.
41. Wheelhouse NM, *et al.* (2006) The effects of macrophage migratory inhibitory factor on acute-phase protein production in primary human hepatocytes. *Int J Mol Med* 18:957–961.
42. Fletcher J, *et al.* (2008) The inhibitory role of stromal cell mesenchyme on human embryonic stem cell hepatocyte differentiation is overcome by Wnt3a treatment. *Cloning Stem Cells*, in press.